Design of an Ultra-Wideband UHF RFID Reader Antenna for Wearable Ankle Tracking Applications

Khodor Jebbawi*, Matthieu Egels, and Philippe Pannier

Abstract—In this paper, a broadband reader antenna is designed and manufactured for wearable ankle strap applications. The frequency range covered for $S_{11} < -10$ dB is from 850 MHz to 1650 MHz with dipole like radiation pattern in free space. The proposed broadband antenna is manufactured with a semi-flex (Taconic RF-35) and flexible (Kapton) substrates. A good agreement between simulations and measurements has been achieved. Prototypes performances have been tested by measuring the reading distance. The maximum reading distance obtained is about 1.46 m at 865 MHz with an output power of the transmitter (P_{TX}) of 25 dBm. Results of functional RFID test show that the proposed antenna can be used as an RFID reader antenna when it is placed on the ankle of the human body.

1. INTRODUCTION

Radio Frequency IDentification (RFID) has evolved over the past few years. Therefore, RFID is becoming increasingly available in a variety of fields, including tracking systems, transportation, warehousing, distribution, retail, healthcare, security, etc. Tracking and monitoring systems using connected RFID devices to provide position and other information is one of the most recent RFID applications. Ankle strap antennas can be an effective solution for tracking systems. In this study, tracking systems based on RFID are used to provide communication between the ankle and a ball in order to recover the statistics of a football match. This application is intended for amateur footballers. Each footballer should be equipped by a sensor. The sensor is composed of an electric circuit related to the proposed antenna [1]. The RFID reader ankle antenna sends a radio frequency signal to the ball equipped with RFID tags to get data that can be used to compute the match statistics. The added value of this study is its contribution in the deployment of RFID systems for complex and extreme environments through proposing RFID antennas capable of operating even when placed on the human body.

There are various wearable antennas that have been developed over the past years. The common design and fabrication techniques for wearable antennas were presented in [2]. The wearable antennas were classified into two main categories: nontextile and fully textile solutions. This classification allows for identifying useful practical guidelines for antenna design. [3] presents the different challenges and issues in designing wearable antennas, their material selection, and fabrication techniques. [4] provides a holistic and critical review of design challenges associated with body-area RFID technologies, including operation frequencies, influence of the surrounding biological tissues, antenna design and miniaturization, and conformance to international safety guidelines. In [5], a flexible thin antenna solution for wearable ankle strap applications with Global Navigation Satellite System (GNSS) and Bluetooth Low Energy (BLE) connectivity is proposed. [6] presents a broadband RFID tag antenna for bio-monitoring applications. [7] presents a wearable UHF RFID reader antenna made of textile materials

and integrated with a work glove. Most of existing techniques such as [7] of designing wearable antennas use ground plane to minimize the influence of the human body on the antenna performance, which makes antenna bulky and not befitting our application, where the sufficiently small form factor is in priority. In addition, the textile solution is generally based on using electro-thread as conductor, but this material has a low electrical conductivity compared to the copper. Weakness in conductivity reduces the read range as well the performance of the antenna.

The high dielectric and loss values of the human tissues reduce the performance of the antenna. The major effects of the human body are: shifting the reflection coefficient (S_{11}) of an antenna to lower frequencies and distortion of the radiation pattern [8–10]. The compensation of this frequency shift in order to keep the antenna matched on 868 MHz can be achieved by reducing the size of the antenna. The value of the gain is proportional with the surface occupied by the antenna, so reducing the antenna size decreases the values of the gain and consequently the reading distance. Therefore, an electrically small antenna is not the best solution. A broadband antenna is an appropriate solution because it is able to compensate the negative effects of the human-tissues [6, 11–13]. In literature, several broadband dipole antennas have been reported. The state of the art on broadband dipole antennas shows that there are two dominant techniques: coupling the dipole by charges (parasitic elements) [14, 15] and charging the prime dipole by elements directly supplied [16, 17]. These techniques cannot be used for our application because the bandwidth of the antennas is less than 50%, which does not satisfy our needs. The use in a standard human ankle (Fig. 2) shifts the antenna operation by 150 MHz downwards, but this value depends on the size of the human ankle. For example, the shifting is more important for a large ankle. Therefore, the bandwidth of the designed antenna should be greater than 50% (UWB) in order to cover all cases (small, standard and large ankles). This main aim of this study is to solve the shifting effect of the human ankle. The gain can be improved by increasing the distance between the antenna and the ankle or by using an electromagnetic wave absorbing materials such as Ferrite but it is so expensive. Improving the gain can be the goal of the future works.

In this paper, a broadband antenna is designed and manufactured for wearable ankle strap applications. The antenna bandwidth is about 64% for a $S_{11} < -10$ dB. The proposed antenna structure consists of a dipole with a triangular F-slot and small rectangle slots.
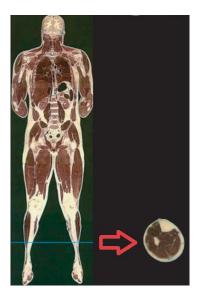
In order to validate the performance of the antenna when it is placed on a human ankle, a functional RFID reading distance test has been carried out by using an RFID Reader module (Red4S [18]) and a tag (Frog 3D [19]) from phychips and smartrac respectively. Results show that the proposed antenna can be used as an RFID reader antenna for wearable applications.

2. HUMAN ANKLE MODEL

Most of designed wearable antennas have been based on electromagnetic models for simulations (3D model [20], homogeneous phantom [21], multi-layer human model [22]). In this work, a heterogeneous electromagnetic model of human ankle is realized based on "Visible Human Project" [23] in order to know the effects of a human ankle on the antenna performances. A tomographic image of the human ankle is extracted from "Visible Human Project" in order to obtain the thicknesses and diameters of different ankle-tissues as shown in Fig. 1. Dielectric features of tissues at 867 MHz can be obtained from [24]. Table 1 shows all parameters used to achieve the model presented in Fig. 2. In order to minimize the effect of the human ankle on the antenna, a space of 2 mm with the rubber silicon

Table 1. Dielectric values of the human tissues at 867 MHz.

Tissue	Skin	Fat	Muscle	Bone
Relative Permittivity (ϵ_r)	41.5	5.47	55.1	20.8
Dielectric loss	0.43	0.19	0.35	0.33
Conductivity (S/m)	0.86	0.05	0.93	0.33

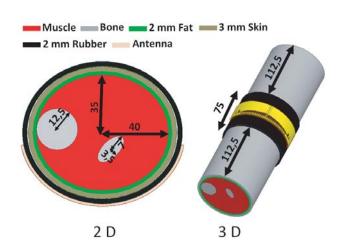**Figure 1.** Tomographic image of a human ankle.

Figure 2. 2D and 3D of the human ankle HFSS model (units: mm).

thickness ($\epsilon_r = 3$, Loss $= 0.01$ [25]) is added between the antenna and the ankle as shown in Fig. 2.

The antenna should be bend to ensure the comfort when it is placed on the ankle. The effect of bending with different angles (30°, 60°, 90°) is discussed in [26]. Results of simulations show that the bending can slightly shift the bandwidth, but the antenna keeps approximately the same response. As the proposed antenna is broadband, the bending cannot affect the antenna performance.

3. ANTENNA DESIGN

The bandwidth of the designed antenna should be greater than 50% to overcome the frequency shifting caused by the human body. In addition, the antenna must cover the UHF RFID band. Firstly, the broadband antenna is designed by using a semi-flex Taconic RF-35 ($\tan \delta = 0.0018$) dielectric substrate with a 3.5 of permittivity and a 1.52 mm of thickness. This substrate is chosen because the prototype can be manufactured rapidly in the laboratory by using LPKF protolaser [27]. Once the desired antenna performance is obtained with Taconic, the second step is manufacturing the proposed antenna with a flexible substrate (Kapton).

The geometry of the proposed antenna is presented in Fig. 3. The designed antenna structure consists of a dipole with a triangular F-slot and small rectangular slots as shown in Fig. 3. The dipole length is about a half of the effective wavelength ($\lambda_{eff}/2$) at the desired resonant frequency. Small rectangular slots were placed on the dipole in order to shift the resonant frequency to lower frequencies and cover the ETSI RFID band (865 MHz $\rightarrow$ 868 MHz) [28].

The optimal geometrical parameters of the antenna are obtained by using ANSYS High-Frequency Structure Simulator (HFSS) version 17. All the detailed parameters of the antenna are summarized in Table 2. As mention in this table, several parameters are defined but their are two main parameters (α and a) that control the performance of the antenna. For that, only two parametric studies are discussed and presented.

Table 2. Parameters of the proposed antenna (units: mm).

L	$L1$	W	$W1$	a	b	c	d	e	f	g	h	α
128.8	63.6	30	29	53.3	7.5	1.3	3.8	4.4	3.8	6.5	3.5	84.2°

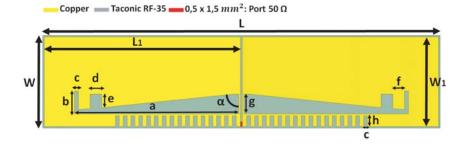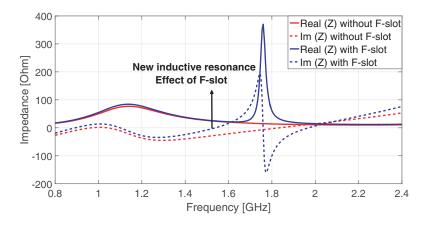**Figure 3.** Geometry of the proposed antenna.

Figure 4. Real(Z) and Im(Z) of the both antennas with and without F-slot.
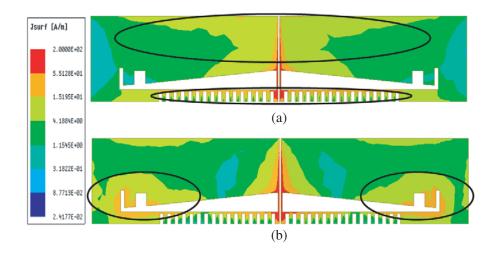

Figure 5. Surface current (a) 868 MHz, (b) 1500 MHz.

Start with the effect of F-slot on the antenna performance. Fig. 4 shows the real and imaginary parts of the impedance against frequency for both antennas with and without F-slot. It is observed that the triangular F-slot adds a new inductive resonant mode at 1.5 GHz (Im(Z) = 0 and Real(Z) is close to 50 Ω).

To verify the impact of F-slot on the dipole, the current distribution of the antenna at the two resonant frequencies is plotted as shown in Fig. 5. It is observed that the most of the current is located on the dipole at 868 MHz, while at the second resonant frequency (1.5 GHz), the magnitude of the current circulated on the F-slot is greater than that on the main dipole. Therefore, the F-slot acts as a

slot-dipole by adding a new mode which resonates at higher frequencies.

The broadband behavior is achieved by coupling the first mode (prime dipole) with the new resonant mode created by F-slot. Modifying the F-slot dimensions does not affect the size of the antenna because F-slot is located in the dipole. Therefore, controlling the resonant frequency of mode 2 is easier than mode 1. The parameters (α and a) can control the resonant frequency of mode 2 in order to couple it with the first mode.

Figure 6 shows S_{11} of the antenna versus frequency with respect to the variation of (a). It is observed that the new resonant mode is shifted to higher frequencies and decoupled from the first resonant mode when the value of (a) decreases, while keeping c fixed.
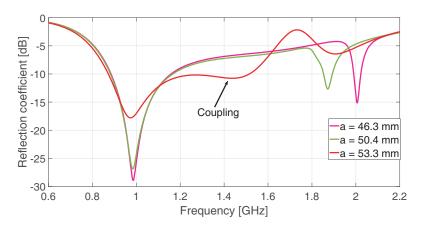

Figure 6. S_{11} of the proposed antenna as the function of frequency respect to the variation of (a).

Figure 7 presents the reflection coefficient of the proposed antenna against frequency with different values of (α). As shown in this figure, the coupling between the first and the new resonant modes is achieved when the value of (α) increases, while e remains fixed. Moreover, the coupling between the two modes is controlled by (α). Therefore, the angle (α) and length of the F-slot (a) affect the antenna performance (bandwidth). In addition, the best coupling (larger bandwidth) is obtained for $\alpha = 84.2°$ and $a = 53.3$ mm.
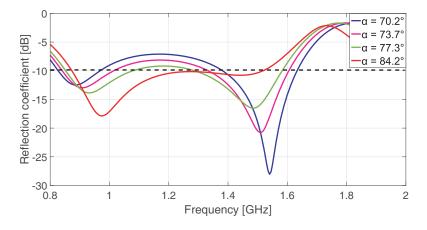

Figure 7. S_{11} of the proposed antenna as the function of frequency with different values of (α).

4. RESULTS AND DISCUSSIONS

The proposed antenna is fabricated using a single metallic layer of Taconic RF-35 ($128.8 \times 30 \times 1.52$ mm^3) as shown in Fig. 8.
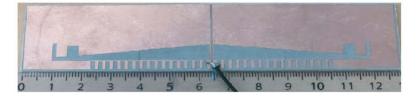
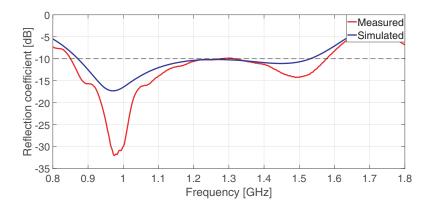**Figure 8.** Photograph of manufactured antenna with Taconic RF-35.

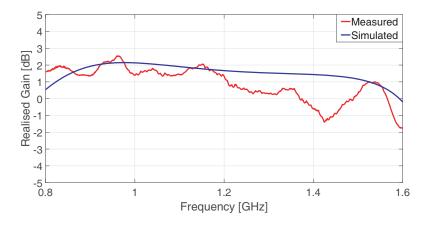**Figure 9.** Simulated and measured S_{11} of the proposed antenna in free space.

Figure 10. Simulated and measured gain of the proposed antenna without human ankle.

The measurement of the reflection coefficient is done using a ZVA24 Network Analyzer. Fig. 9 shows simulated and measured reflection coefficients of the proposed antenna as a function of frequency in free space. The measured results are in good agreement with the predicted simulated ones. Results obtained indicate that the antenna covers a 660 MHz broadband for $S_{11} < -10$ dB.

Graphs of measured and simulated gains versus frequency of the proposed antenna in free space are plotted in Fig. 10. The antenna has a good gain ($\simeq 2$ dBi) in the operating band (865 MHz to 1525 MHz).

The radiation patterns of the fabricated antenna are measured in a standard far-field anechoic chamber. The measured and simulated E-plane and H-plane radiation patterns at 868 MHz of the antenna without ankle are presented in Fig. 11. The results show that the antenna has a dipole like radiation pattern as expected.

Figure 12 presents the simulated and measured S_{11} of the antenna when it is placed on the human ankle. The antenna remains matched to 868 MHz when it is placed at 2 mm from the ankle. The slightly
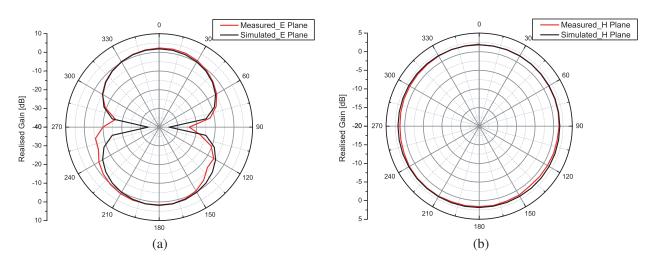
Figure 11. Simulated and measured (a) E-plane, (b) H-plane of the proposed antenna in free space at 868 MHz.
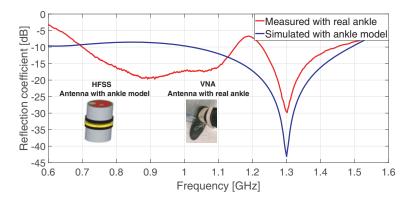

Figure 12. Simulated and measured S_{11} of the antenna with human ankle.

different values between the simulation and measurements are due to the variation of the human ankle parameters (thickness, diameter, etc.) from one individual to another. This variation of characteristics of human tissues has an impact on the impedance of the antenna as well on reflection coefficient.

The effect of the human ankle on the antenna radiation patterns is shown in Fig. 13. This figure displays the simulated 3D radiation patterns of the antenna with and without model ankle. Fig. 13(b) presents the 3D radiation patterns of the antenna in free space. It is observed that the antenna has a dipole radiation pattern at 868 MHz. Fig. 13(a) shows the 3D radiation patterns of the antenna with ankle at 868 MHz. Results of simulation indicate that the radiation pattern of the antenna is more directive and exhibit a hemispherical radiation pattern when it is placed on the human ankle. It is due to the higher loss values of the human tissues. For the performance, the antenna gain is reduced by 11 dB when it is placed at 2 mm from the ankle.

The gain drop is dependent on the characteristics (dimensions, loss, ϵ_r) of the ankle. In addition, the distance between the antenna and the ankle is a main factor that affects the value of the gain drop. To illustrate the impact of the distance, the radiation pattern of the antenna placed at 10 mm from the ankle is simulated. Fig. 14 shows the simulation results. The gain drop is 7 dB for 10 mm of distance. Therefore, increasing the distance between the antenna and the ankle reduces the value of the gain drop.

In order to achieve more flexibility, a different substrate is used to manufacture the antenna. This substrate is Kapton ($\epsilon_r = 3.5$; $\tan(\delta) = 0.0026$) with thickness of 0.1 mm [29]. The size of the antenna is conserved, and only the length of F-slot is changed to match the dielectric constant of the new substrate.
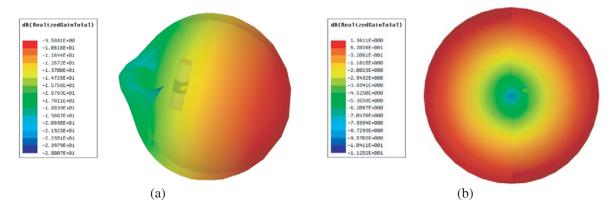
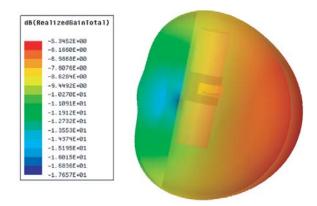**Figure 13.** Simulated 3D radiation patterns of the proposed antenna (a) with, (b) without ankle at 868 MHz.

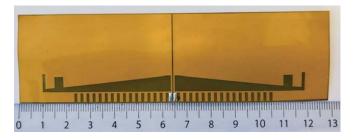**Figure 14.** Simulated 3D radiation patterns with 10 mm of distance.

Figure 15. Photograph of manufactured antenna with Kapton.

Fig. 15 displays a photograph of the flexible broadband antenna. The simulated and measured results of reflection coefficient and gain of the flexible antenna in free space are illustrated in Fig. 16. The two prototypes (Taconic and kapton) present the same mechanism of radiation. Moreover, the results indicate that the bandwidth of the antenna with Kapton (800 MHz) is larger than the one with Taconic RF-35 (660 MHz). It is due to the high thickness of the Taconic (1.52 mm) compared to the Kapton (0.1 mm).

The Fractional Bandwidth (FBW) of an antenna is a parameter used to classify the antenna bandwidth (narrowband, wideband or ultra-wideband). Narrowband antennas typically have an FBW less than 10%, while the FBW of a wideband antennas is 20% or more. Antennas with an FBW greater than 50% are referred as ultra-wideband antennas. A comparison is done between the FBW of the proposed antennas and the other antennas from the state of art. The selection criteria of the antennas
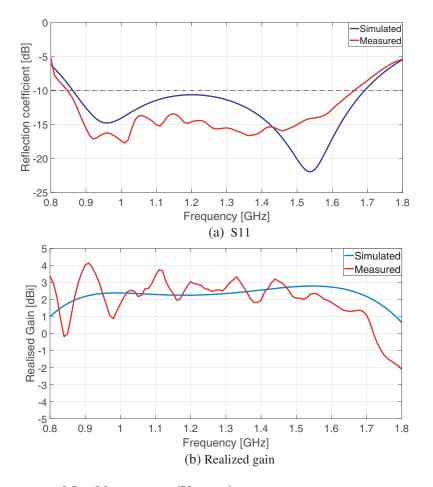
(a) S11

(b) Realized gain

Figure 16. Performance of flexible antenna (Kapton).

included in the literature are: operate in the ETSI band, have the same type (dipole), and presented as a broadband antennas. Results of comparison are shown in Table 3. The proposed antennas (Kapton and Taconic) have an FBW greater than 50%, where the FBWs of the other antennas are between 15 and 30%. Therefore, the antennas in the literature are wideband, and the proposed antenna is considered as an ultra-wideband antenna.

Finally, the manufactured antennas are tested with the human ankle by measuring the reading distance at different values of power. As shown in Fig. 17, the measurement is taken by using a UHF RFID reader module (Red4S [18] from phychips) and a UHF RFID tag (Frog 3D [19] from smartrac).

Table 3. Comparison to state of art.

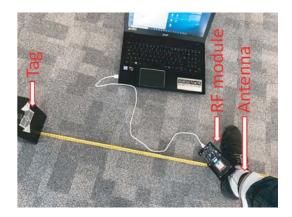| Reference	Surface	Bandwidth
[14]	2.064 dm^2	16.2%
[15]	9.3 dm^2	27.1%
[16]	0.267 dm^2	19%
[17]	0.341 dm^2	23.9%
[30]	2.89 dm^2	25.3%
Paper: Taconic RF-35	0.386 dm^2	55.2%
Paper: Kapton	0.386 dm^2	64%

Figure 17. Photography of RFID functional reading distance test of the proposed antenna when it is placed on the human ankle.

Table 4. Results of the RFID functional reading distance test.

Power (dBm)	Read range	
	Taconic	Kapton
13	45 cm	48 cm
16	72 cm	74 cm
20	97 cm	101 cm
25	145 cm	146 cm

As shown in Table 4, both the broadband antennas present good reading distance values on the human ankle. Hence, it indicates that the proposed antenna is useful for wearable ankle strap applications.

5. CONCLUSION

In this study, an ultra-wideband UHF RFID dipole antenna is presented. The performance of the antenna is investigated and analyzed in free space and when it is placed on the human ankle. The tested reading distance shows that the proposed antenna can be used as an RFID reader antenna for wearable ankle strap applications.

REFERENCES

1. "RFID system for amateur footballers," https://www.youtube.com/watch?v=Woa7mqThYgc.
2. Corchia, L., G. Monti, and L. Tarricone, "Wearable antennas: Nontextile versus fully textile solutions," *IEEE Antennas and Propagation Magazine*, Vol. 61, No. 2, 71–83, 2019.
3. Paracha, K. N., S. K. A. Rahim, P. J. Soh, and M. Khalily, "Wearable antennas: A review of materials, structures, and innovative features for autonomous communication and sensing," *IEEE Access*, Vol. 7, 56694–56712, 2019.
4. Kiourti, A., "RFID antennas for body-area applications: From wearables to implants," *IEEE Antennas and Propagation Magazine*, Vol. 60, No. 5, 14–25, 2018.
5. Flores-Cuadras, J. R., J. L. Medina-Monroy, R. A. Chavez-Perez, and H. Lobato-Morales, "Flexible thin antenna solution for wearable ankle bracelet applications with GNSS and BLE connectivity," *Microwave and Optical Technology Letters*, Vol. 60, No. 5, 1239–1245, 2018.
6. Marques, D., M. Egels, and P. Pannier, "Broadband UHF RFID tag antenna for bio-monitoring," *Progress In Electromagnetics Research B*, Vol. 67, 31–44, 2016.

7. Ahmed, S., A. Mehmood, L. Sydänheimo, L. Ukkonen, and T. Björninen, "Glove-integrated textile antenna with reduced sar for wearable UHF RFID reader," *2019 IEEE International Conference on RFID Technology and Applications (RFID-TA)*, 231–235, IEEE, 2019.

8. Psychoudakis, D. and J. L. Volakis, "Conformal asymmetric meandered are (AMF) antenna for body-worn applications," *IEEE Antennas and Wireless Propagation Letters*, Vol. 8, 931–934, 2009.

9. Garcia-Pardo, C., C. Andreu, A. Fornes-Leal, S. Castelló-Palacios, S. Perez-Simbor, M. Barbi, A. Vallés-Lluch, and N. Cardona, "Ultrawideband technology for medical in-body sensor networks: An overview of the human body as a propagation medium, phantoms, and approaches for propagation analysis," *IEEE Antennas and Propagation Magazine*, Vol. 60, No. 3, 19–33, 2018.

10. Fortino, G. and Z. Wang, *Advances in Body Area Networks I: Post-conference Proceedings of Bodynets 2017*, 2017.

11. Lovett, T., J. Flint, D. S. Fonseca, and I. H. Daniel, "Novel broadband antenna for wearables," *2014 Loughborough Antennas and Propagation Conference (LAPC)*, 178–181, IEEE, 2014.

12. Gandhimohan, J. and T. Shanmuganantham, "CPW fed bud shaped antenna with DGS in UWB range for body area network," *2017 IEEE International Conference on Antenna Innovations & Modern Technologies for Ground, Aircraft and Satellite Applications (iAIM)*, 1–3, IEEE, 2017.

13. Kod, M., J. Zhou, Y. Huang, R. Alrawashdeh, and M. Hussein, "A dual broadband butter y loop antenna for body wearable applications," *2015 Loughborough Antennas & Propagation Conference (LAPC)*, 1–3, IEEE, 2015.

14. Keyrouz, S. and H. Visser, "Efficient direct-matching rectenna design for RF power transfer applications," *Journal of Physics: Conference Series*, Vol. 476, 012093, IOP Publishing, 2013.

15. Turkmen, C., Y. Bakirli, M. Secmen, and M. Altuntas, "Printed quasi yagi antenna with closely spaced and thick directors for triple ISM-band/wideband applications at UHF," *2018 IEEE International Symposium on Antennas and Propagation & USNC/URSI National Radio Science Meeting*, 677–678, IEEE, 2018.

16. Zeng, R.-H. and Q.-X. Chu, "A broadband antenna for multi-standard UHF RFID tag applications," *2010 International Conference on Microwave and Millimeter Wave Technology*, 1898–1900, IEEE, 2010.

17. Sabaawi, A. M. and K. M. Quboa, "Wideband modified dipole antenna for passive UHF RFID tags," *2010 7th International Multi-Conference on Systems, Signals and Devices*, 1–4, IEEE, 2010.

18. "Red4s," http://www.phychips.com/product-red/.

19. "Smartrac," https://www.smartrac-group.com/frog-3d.html.

20. Amani, N., A. Jafargholi, and R. Pazoki, "A broadband VHF/UHF-loaded dipole antenna in the vicinity of a human body," *IEEE Transactions on Antennas and Propagation*, Vol. 65, No. 10, 5577–5582, 2017.

21. Bashir, Z., M. Zahid, N. Abbas, M. Yousaf, S. Shoaib, M. A. Asghar, and Y. Amin, "A miniaturized wide band implantable antenna for biomedical application," *2019 UK/China Emerging Technologies (UCET)*, 1–4, IEEE, 2019.

22. Sharif, A., J. Ouyang, H. T. Chattha, M. A. Imran, and Q. H. Abbasi, "Wearable UHF RFID tag antenna design using Hilbert fractal structure," *2019 UK/China Emerging Technologies (UCET)*, 1–3, IEEE, 2019.

23. "Visible human project," https://www.imaios.com/en/e-Anatomy/Thorax-Abdomen-Pelvis/Visible-Human-Project!.

24. http://niremf.ifac.cnr.it/tissprop/htmlclie/htmlclie.php.

25. "Dielectric-chart," http://www.eccosorb.com/Collateral/Documents/English-US/dielectric-chart.pdf.

26. Liu, R., H. Zheng, Z. Song, L. Wang, W. Cui, M. Wang, and E. Li, "Design of wideband and flexible implantable antenna for wireless medical application," *2019 IEEE 2nd International Conference on Electronic Information and Communication Technology (ICEICT)*, 732–734, IEEE, 2019.

27. "Lpkf protolaser," http://www.electronique-mag.com/article1080.html.

28. "Etsi," http://www.etsi.org/technologies-clusters/technologies/radio/RFID.

29. "Datasheet of kapton," https://www.dupont.com/content/dam/dupont/products-and-services/membranes-and-films/polyimde-films/documents/DEC-Kapton-summary-of-properties.pdf.

30. Wei, X.-D., H.-L. Zhang, and B.-J. Hu, "Novel broadband center-fed UHF near-field RFID reader antenna," *IEEE Antennas and Wireless Propagation Letters*, Vol. 14, 703–706, 2014.